



ELSEVIER

Inorganica Chimica Acta 339 (2002) 193–201

**Inorganica
Chimica Acta**

www.elsevier.com/locate/ica

Interaction between Glyglu and Ca^{2+} , Pb^{2+} , Cd^{2+} and Zn^{2+} in solid state and aqueous solution.

Crystal structures of poly[aqua-1,2- κ -O-di[lead(glygluH)]bis(perchlorate)] and poly[bisglycylglutamic-cadmium(II) tetrahydrate]

Rosana Ferrari^a, Sylvain Bernés^b, Cecilia R. de Barbarín^c, Guillermo Mendoza-Díaz^d,
Laura Gasque^{a,*}

^a Departamento de Química Inorgánica, Facultad de Química, Universidad Nacional Autónoma de México, Ciudad Universitaria, México, D.F. 04510, Mexico

^b Centro de Química, Instituto de Ciencias, B. Universidad Autónoma de Puebla, Apartado Postal 1613, Puebla, Pue., Mexico

^c Facultad de Ciencias Químicas, Universidad Autónoma de Nuevo León, Monterrey, N.L., Mexico

^d Facultad de Química, Universidad de Guanajuato, Noria Alta s/n, Guanajuato, Gto. 36050, Mexico

Received 6 November 2001; accepted 23 April 2002

Dedicated to Professor Dr. H. Sigel on the occasion of his 65th birthday, while thanking him for many years of inspiring work and encouraging comments.

Abstract

Glycylglutamic acid (GEH_2) is a peptide usually present in calcium binding sites. The interaction between the peptide and the cations Ca^{2+} , Pb^{2+} , Cd^{2+} , and Zn^{2+} in aqueous solution and in the solid state is described. Six compounds were isolated with different protonation states of the ligand. Potentiometric equilibrium studies, ^{13}C and ^{111}Cd solid state CP MAS NMR and IR spectroscopy were performed. Two crystal structures are reported: $[\text{Pb}(\text{GEH})(\text{H}_2\text{O})_{1/2}]\text{ClO}_4$ and $[\text{Cd}(\text{GEH})_2]\cdot 3\text{H}_2\text{O}$. Both constitute 3D polymers, where only carboxylate groups are coordinated to the cations. The crystalline lead compound shows a hemidirected coordination sphere due to its stereochemically active lone pair. In deprotonated derivatives, it is possible to assign a metal-amino interaction to a far IR signal ($340\text{--}370\text{ cm}^{-1}$).

© 2002 Elsevier Science B.V. All rights reserved.

Keywords: Glycylglutamic acid; Cations; Spectroscopy; Equilibrium; Structures

1. Introduction

The protein responsible for calcium transport and uptake in mammalian intestine, calbindin $\text{D}_{9\text{K}}$ [1], is also related to the assimilation of lead [2], zinc [3] and cadmium [4].

Due to its similarity in radius to Ca^{2+} , Cd^{2+} has been widely used as a tool to study calcium binding sites in many systems [5], as it frequently presents analogous geometries to those of calcium.

Most of the studies regarding these cations associated to the protein, are in vivo or in vitro studies performed on the whole protein, and do not yield information about the coordination behavior of the protein toward each cation. As a first attempt to understand the similarities and differences in the coordination of each system, we decided to model the binding site by using the most frequent aminoacids present in the EF hands from most calcium binding proteins, aspartate [6] and glutamate. Secondly, we studied the solution equilibria and the structural properties of the coordination compounds formed by the dipeptide Glyglu (from now on referred to as GE^{2-} , GEH^- or GEH_2 , depending on its

* Corresponding author. Tel./fax: +555-622-3811

E-mail address: gasquel@servidor.unam.mx (L. Gasque).

protonation state) and the cations Ca^{2+} , Pb^{2+} , Cd^{2+} and Zn^{2+} . This dipeptide is widely found in calcium binding sites of EF-hand-proteins [1b, 7].

2. Experimental

2.1. Potentiometric determinations

All pH calibrations were performed with standardized HCl aqueous solutions to measure hydrogen ion concentrations directly ($\text{pH} = -\log[\text{H}^+]$). Ionic strength was imposed to 0.1 M with KNO_3 . Titrations of the ligand in the absence or presence of metal ions in aqueous solution were conducted in a standard way. Cell solutions (50.00 ml) were purged with a purified nitrogen flux stream. Experimental runs were carried out by adding increments of standardized approximately 0.1 N NaOH to a solution containing GEH_2 plus other components (KNO_3 solution, metal solution and an excess of HCl). The concentrations of the sample solutions were $5 \times 10^{-2} \text{ M}$ for GEH_2 ; the 1:1 metal:ligand systems were prepared by adding the required volume from the corresponding cation standard solutions (Titrisol®). The titrations of M-GEH_2 in a 1:1 ratio, were carried out to investigate the mononuclear 1:1 complexes. The pH range for accurate measurements was considered to be 2–11 in the case of the free ligand and the calcium–ligand solution; for the other cations upper pH limit was established according to the precipitation observed. The $\text{p}K_w$ value for the aqueous system, defined as $-\log([\text{H}^+][\text{OH}^-])$ was considered to be 13.78 at the mentioned ionic strength and temperature conditions (25 °C), as indicated by Jameson and Wilson [8].

Protonation constants and stability constants were calculated from the potentiometric data with the HYPERQUAD 2000NT program [9]. The error in the constants listed in Table 2 is estimated as ± 0.04 log units on the basis of the σ_{fit} value, which measures the deviation of the experimental curve and the curve calculated from the equilibrium constants, being less than 0.01 pH unit in all potentiometric determinations. Species distribution diagrams were computed from the measured equilibrium constants and plotted with MEDUSA [10].

2.2. Physical measurements

A Metrohm 702 Titrino set including digital pH meter coupled to a PC, and fitted with a Metrohm Ag–AgCl combined electrode, was used for potentiometric titrations. Each aqueous sample was contained in a 75 ml jacketed glass cell thermostated at 25.00 (± 0.05) °C using a circulating constant-temperature water bath.

Elemental analyses were carried out by Desert Analytics, Tucson, AZ.

Powder X-ray diffraction was performed in a SIEMENS D5000, using Cu radiation of $\lambda = 1.5406 \text{ nm}$ and scintillation counter.

IR spectra were recorded in the 4000–400 cm^{-1} region using KBr pellets in a Nicolet 540 spectrophotometer. The far IR spectra were recorded in a Nicolet 740 FTIR spectrophotometer in the 700–70 cm^{-1} region using polyethylene pellets. Amino group protons were interchanged with deuterium, isolating the compounds from D_2O solutions.

The CP MAS NMR spectra were recorded on a Varian Unity-plus 300 MHz spectrometer operating at 75.429 MHz for ^{13}C and 63.602 MHz for ^{111}Cd , and 30° pulses were used. A 7 mm diameter silicon nitride rotor with kel-F caps was used as container. For ^{13}C spectra, the rotor spin rate was kept between 3.5 and 4.5 kHz for all experiments, with a delay time of 7 s, and between 128 and 516 transients accumulated. Adamantane was used as external reference. For ^{111}Cd spectra, the rotor spin rate was kept between 3.5 and 5 kHz for all experiments, with a delay time between 5–10 s and between 500 and 10 000 transients were accumulated, contact time for cross polarization was set between 1–2.5 ms and 0.05 s for acquisition time. CdCO_3 was used as external reference. Spectra were recorded using total side band suppression when side bands were not well removed by spinning. Processing was made using a 20–40 Hz of line broadening.

2.3. Preparation of $\text{Ca}(\text{GEH})\text{Cl}\cdot 2\text{H}_2\text{O}$ (I)

Five millimole of calcium chloride were dissolved in 10 ml of water and 5 mmol of glycylglutamic acid were added. The pH was adjusted to 5 with 1 M NaOH. Methanol was added in a 5:1 proportion in order to induce the precipitation of the product. A white hygroscopic powder was filtered. *Anal.* Found: C, 27.48, H, 4.76, N, 8.62. Calc. for $\text{Ca}(\text{C}_7\text{H}_{11}\text{O}_5\text{N}_2)\text{Cl}\cdot 2\text{H}_2\text{O}$: C, 26.71, H, 4.8, N, 8.9%.

2.4. Preparation of $\text{Pb}(\text{GEH})(\text{ClO}_4)$ (II)

Five millimole of lead perchlorate were dissolved in 50 ml water and combined with 5 mmol of glycylglutamic acid in 50 ml of water. pH was adjusted to 4.3 with 0.1 M NaOH and the solution was left standing. Colorless needles were collected after a week. *Anal.* Found: C, 16.04, H, 2.3, N, 5.33. Calc. for $\text{Pb}(\text{C}_7\text{H}_{11}\text{O}_5\text{N}_2)\text{ClO}_4\cdot 1/2\text{H}_2\text{O}$: C, 16.21, H, 2.33, N, 5.4%.

2.5. Preparation of $\text{Pb}(\text{GE})$ (III)

Five millimole of glycylglutamic acid were dissolved in 300 ml water and 1.115 g of PbO powder (litharge) were added gradually. The reaction vessel was placed in an ultrasound bath for 15 min during which the yellow

powder turned into a white precipitate. *Anal.* Found: C, 17.99, H, 2.10, N, 5.79. Calc. for $[\text{Pb}(\text{C}_7\text{H}_{10}\text{N}_2\text{O}_5)] \cdot 1/4\text{PbO}$: C, 18.01, H, 2.17, N, 6.02%.

2.6. Preparation of $\text{Cd}(\text{GE})$ (IV)

Five millimole of cadmium nitrate were dissolved in 50 ml water and combined with 5 mmol of glycylglutamic acid also in 50 ml of water. pH was adjusted to 7 with 0.1 M NaOH and a precipitate formed. The filtrate was left overnight at 100 °C. *Anal.* Found: C, 26.61, H, 3.33, N, 8.68. Calc. for $\text{Cd}(\text{C}_7\text{H}_{10}\text{O}_5\text{N}_2)$: C, 26.73, H, 3.2, N, 8.91%.

2.7. Preparation of $\text{Cd}(\text{GEH})_2 \cdot 3\text{H}_2\text{O}$ (V)

Five millimole of glycylglutamic acid were dissolved in 300 ml water. Only 1.665 mmol of CdO powder dissolved in this solution by periodically placing the reaction vessel in an ultrasound bath every 15 min until

it was no longer possible to dissolve the brown oxide, but just turned into white. The solid was filtered off and the solution left to crystallize for 2 days under a vacuum yielding colorless irregular crystals. *Anal.* Found: C, 28.7, H, 5.04, N, 9.71. Calc. for $\text{Cd}(\text{C}_7\text{H}_{11}\text{O}_5\text{N}_2)_2 \cdot 3\text{H}_2\text{O}$: C, 29.35, H, 4.93, N, 9.78%.

2.8. Preparation of $\text{Zn}(\text{GE})$ (VI)

Five millimole of zinc nitrate were dissolved in 50 ml water and combined with 5 mmol of glycylglutamic acid in 50 ml of water. pH was adjusted to 7 with 0.1 M NaOH and a precipitate is formed. The white solid was vacuum filtered and dried. *Anal.* Found: C, 29.56, H, 4.1, N, 9.88. Calc. for $\text{Zn}(\text{C}_7\text{H}_{10}\text{O}_5\text{N}_2)$: C, 29.44, H, 4.24, N, 9.81%.

2.9. Crystallography

Single-crystal X-ray diffraction data for **II** and **V** were measured at 298 K at 0.71 Å resolution, on a Bruker P4 diffractometer, using common procedures [11]. A correction for absorption was applied for both complexes, based on ψ -scans with χ close to 90°. The structures were solved and refined using standard procedures [12], with neither restraints nor constraints. For **II**, H atoms H5 (secondary amine group) and H15A (coordinated water molecule) were found on difference maps. Non-coordinated water molecules were found in compound **V**, two of which are disordered with site occupation factors fixed to 1/4 (O51 and O52). H atoms for these molecules were found on difference maps. In both cases, H atoms were refined using a Riding model with fixed isotropic thermal parameters. The refinement of a Flack parameter [13] confirmed the absolute configuration of the enantiopure GEH ligand in **II** and **V** to be C4-*S*, as expected. For **II**, a somewhat high peak, 1.51 e Å⁻³, was observed in the last Fourier map, which accounts for the difficulty in applying an accurate absorption correction. Selected crystal data are collected in Table 1.

Table 1
Crystal data

	II	V
Empirical formula	PbC ₇ H ₁₂ ClN ₂ O _{9.5}	CdC ₁₄ H ₂₈ N ₄ O ₁₃
Formula weight	518.83	572.80
Crystal system	monoclinic	trigonal
Color, habit	colorless, needle	colorless, block
Crystal size (mm)	0.42 × 0.06 × 0.04	0.70 × 0.70 × 0.52
Space group	C2	P3 ₂ 21
<i>a</i> (Å)	18.865(2)	13.1931(7)
<i>b</i> (Å)	4.9210(10)	
<i>c</i> (Å)	14.197(2)	11.3498(8)
β (°)	103.720(10)	
<i>Z</i>	4	3
Absorption coefficient (mm ⁻¹)	13.438	1.027
Radiation	Mo K α (λ = 0.71073 Å)	Mo K α (λ = 0.71073 Å)
2 θ Range (°)	4.44–60.00	3.56–60.00
Reflections collected	2660	4957
Independent reflections ^a	2460 (R_{int} = 3.46%)	3261 (R_{int} = 2.74%)
Transm. Factors (min., max.)	0.100, 0.153	0.509, 0.608
Final <i>R</i> [2156I > 2 σ (I)] (%) ^{a,b}	R_1 = 3.65, wR_2 = 8.06	R_1 = 2.70, wR_2 = 7.43
Final <i>R</i> (all data) (%) ^{a,b}	R_1 = 4.86, wR_2 = 8.59	R_1 = 2.78, wR_2 = 7.49
Goodness-of-fit, <i>S</i> ^a	1.030	1.042
Data-to-parameters ratio	2460/187	3261/161

^a R_{int} , R_1 , wR_2 and *S* are defined as follows: $R_{\text{int}} = \sum |F_o^2 - \langle F_o^2 \rangle| / \sum F_o^2$, $R_1 = \sum |F_o| - |F_c| / \sum |F_o|$, $wR_2 = \sqrt{\sum w(F_o^2 - F_c^2)^2 / \sum w(F_o^2)^2}$,

$S = \sqrt{\sum w(F_o^2 - F_c^2)^2 / m - n}$.

^b Weighting schemes: $w = [\sigma^2(F_o^2) + (0.364P)^2 + 7.7015P]^{-1}$ for **II**, $w = [\sigma^2(F_o^2) + (0.0460P)^2 + 0.3262P]^{-1}$ for **V**, where $P = (\max [F_o^2, 0] + 2 F_c^2) / 3$.

Table 2
Equilibrium constants calculated from experimental data

Cation	β_{101} ^a	β_{111} ^b	p <i>K</i> _a amine group ^c	$K_{\text{M,LLH}}^{\text{MLH}}$ ^d
Ca ²⁺	2.67(3)	10.57(4)	7.90	2.197(42)
Pb ²⁺	3.89(2)	10.70(3)	6.81	2.327(32)
Zn ²⁺	3.98(2)	9.96(6)	5.98	1.587(62)
Cd ²⁺	3.426(7)	9.99(1)	6.564	1.617(12)

^a β_{101} : $\text{GE}^{2-} + \text{M}^{2+} \rightleftharpoons [\text{MGE}]$.

^b β_{111} : $\text{GE}^{2-} + \text{H}^+ + \text{M}^{2+} \rightleftharpoons [\text{M}(\text{GEH})]^+$.

^c p*K*_a: $[\text{M}(\text{GEH})]^+ \rightleftharpoons [\text{MGE}] + \text{H}^+$.

^d $K_{\text{M,LLH}}^{\text{MLH}}$: $\text{M}^{2+} + \text{GEH}^- \rightleftharpoons [\text{M}(\text{GEH})]^+$.

3. Results and discussion

3.1. pH-potentiometric study

The fully protonated species in the ligand is designated as GEH_3^+ and the fully deprotonated species as GE^{2-} . The pK_a values obtained in this work for its three successive stepwise protonations, 8.373(2), 4.450(4) and 2.880(4), are in good agreement with previous report [14].

Metal complex formation studies were performed with approximately 1:1 metal to ligand ratio. Although formation of the 1:2 complexes was allowed for the models, those that exclusively including the MH_xL^x ($x = 0-1$) species, i.e. the 1:1 complex, gave satisfactory statistical fits of the pH data.

The presence of the ligand does not affect the pH value at which the metal hydroxide precipitates (see Fig. 1). Potentiometric data interval was limited to one pH unit prior to that for which precipitation was observed.

$K_{M,LH}^{MLH}$ can be related to the affinity of these cations toward oxygen donors. Both Ca^{2+} and Pb^{2+} ions exhibit a higher affinity toward O than Zn^{2+} and Cd^{2+} ions. For the latter two, the most stable species are those formed by the fully deprotonated ligand. The highest formation constant was found for Zn. This can be directly related to the affinity that these cations, Zn^{2+} and Cd^{2+} , show toward N. The acidity of the terminal ammonium group is enhanced by the formation of the Zn and Cd complexes (see species distribution diagrams, Fig. 1). This is consistent with the fact that preparation of these compounds yields the fully deprotonated ligand derivatives for this two cations while for Pb product isolated and crystallized is the monoprotonated derivative.

It is possible to calculate the formation constant for $Pb(GE)$, even though it is almost absent in solution at the concentrations used (see Fig. 1); this species was isolated from the heterogeneous reaction between a suspension of PbO and a GEH_2 solution (see Section 2.7). Interestingly, the analogous reaction between CdO and a GEH_2 solution yielded the monoprotonated derivative in a 1:2 proportion (see Section 2.9). Attempts to isolate $MGEH^+$ from solution with Zn and Cd led to solids with non-stoichiometric amounts of water molecules.

3.2. NMR spectra

3.2.1. ^{111}Cd CP MAS NMR spectra

A general trend for Cd nuclei chemical shifts has been described [15,16] as an ancillary technique in the determination of the coordination environment on a cadmium atom: shielding on a Cd atom is, (i) decreased when it is bonded to nitrogen (low field shift); (ii)

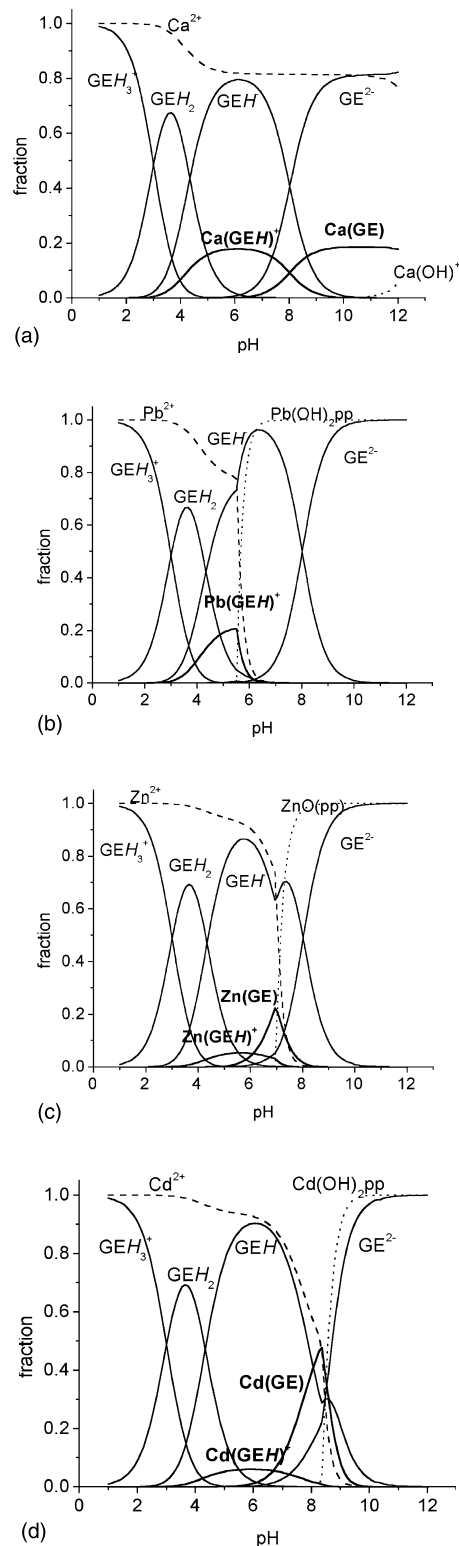


Fig. 1. Species distribution diagram based on total ligand concentration.

increased when bonded to oxygen (high field shift), but (iii) decreased when it is part of a chelate ring.

Compound IV ($CdGE$) has a positive isotropic chemical shift of 92.83 ppm referred to $Cd(ClO_4)_2$,

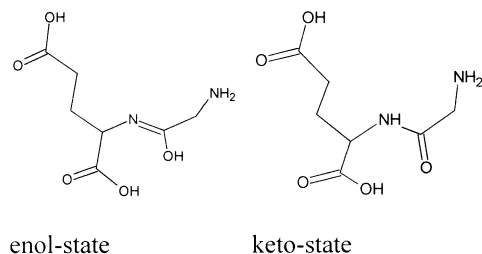


Fig. 2. Scheme of the tautomeric species corresponding to the GlyGluH₂.

which is indicative of nitrogen coordination [17]. It shows a triplet pattern due to the coupling between ¹¹¹Cd and one ¹⁴N. The quadrupolar interaction shifts the axis of quantization on the ¹⁴N away from the direction of the applied magnetic field and thus the dipolar coupling is not completely removed by magic angle spinning [18]. The values of *J* and *S* can be calculated by the separation of the signals, yielding *J* = 110.66 Hz and *S* = 26.08 Hz.

On the other hand, there is a single signal in the ¹¹¹Cd CP MAS spectrum for compound V (Cd(GEH)₂·3H₂O) with a chemical shift of −66.89 ppm referred to Cd(ClO₄)₂. This is consistent with a coordination sphere of oxygen donor atoms exclusively. X-ray diffraction shows that this compound has eight oxygen atoms forming four membered chelates rings bonded to Cd. An increased shielding was expected due to this donor environment (8O). However, the value observed is not as negative as that for other 8O complexes (Cd(NO₃)₂·4H₂O, δ = −100 ppm) [17], and can be explained in terms of the chelating nature of the bonds formed.

3.2.2. ¹³C CP MAS NMR spectra

The free ligand solid-state spectrum yields almost twice as many signals (thirteen) than the expected (seven). This can possibly be attributed to the existence of two tautomeric species, the keto-state and the enol-state (see Fig. 2). Full assignment of the ¹³C CP MAS spectrum for the free ligand would require more experiments which are beyond the scope of this work.

The compounds studied can be grouped into those that have a δ value for the amide carbonyl signal appearing above 170 ppm or below this value (see Table 3). The former set of compounds correspond to the fully deprotonated ligand, whereas the latter corresponds to the monoprotinated derivatives. Both have only one signal in this area, which is the smallest signal in the spectrum. Metal complex formation favors the existence of only one tautomer and would account for the disappearance of the various signals observed for the free ligand.

Complexation has an effect in the relaxation process of the molecule, so further experiments were carried out to measure ¹H relaxation times $\langle T_1 \rangle$ by observing the

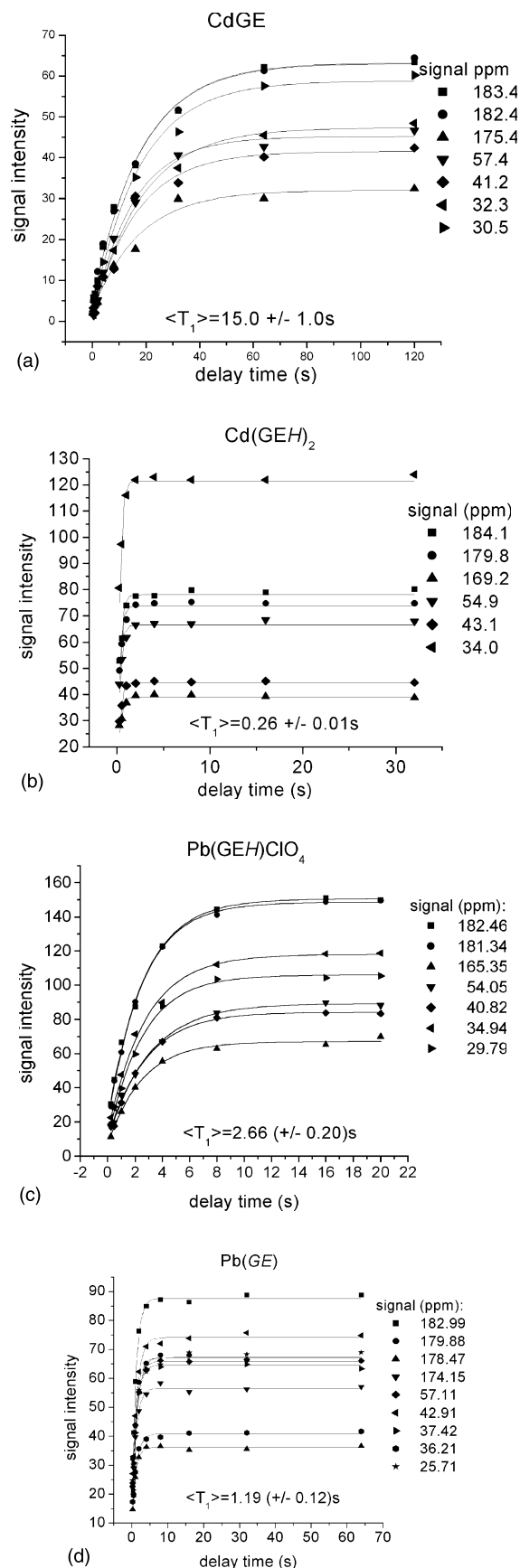


Fig. 3. Effect of the relaxation time in the intensity of the ¹³C CP MAS signals.

Table 3
 ^{13}C CP MAS NMR chemical shifts (ppm) of GlygluH₂ and its derivatives

Nucleus	GEH ₂ free ligand		CaGEHCl(I)	Pb(GEH)ClO ₄ (II)	PbGE(III)	Cd(GE)(IV)	Cd(GEH) ₂ (V)	ZnGE(VI)
CH ₂ G _α	40.8	38.7	42.5	40.8	42.9	41.2	43.1	41.1
CO _G	171.0	167.0	168.9	165.4	174.2	175.4	169.2	174.4
CH _E α	55.1	56.3	56.4	54.0	57.2	57.4	54.9	56.4
COO _E	176.7	180.2	181.9 ^a	182.5	183.0	183.4	184.1	183.7
CH ₂ E _β	25.1	28.0	34.0 ^a	29.8	25.7	30.5	34.0	29.7
CH ₂ E _γ	29.2	33.1	34.0 ^a	34.9	37.4 ^b	32.3	34.0	31.4
COO _E γ	176.7	179.3	181.9 ^a	181.4	179.9 ^b	182.4	179.8	180.2

^a Broad signal.

^b Split signal.

variations in signal intensity for cross-polarization ^{13}C solid state spectra as a function of delay time [19,20] (Fig. 3). The trend in proton $\langle T_1 \rangle$ relaxation times follows the degree of flexibility in the proton containing parts of the molecule.

A significant difference in ^1H relaxation times is observed for the cadmium complexes (see Fig. 3(a and b)). Cd(GE)(IV) which presumably will have chelate rings that include the metal-amino interaction observed by far IR and described below, has a ^1H relaxation time of $\langle T_1 \rangle = 15 \pm 1$ s, while compound V, Cd(GEH)₂·3H₂O, has a $\langle T_1 \rangle$ of 0.26 ± 0.01 s. The latter compound has bridging ligands and very loose water molecules (according to the X-ray results) which are capable of assisting the relaxation process. Values below one second are off the limit of our determinations due to the few data points collected in this interval.

For both forms of the free ligand, relaxation times are also less than 1 s. This also holds for the calcium complex (I), as was expected for an interaction that is mainly ionic and weak enough to allow for rapid relaxation of the ligand.

A somewhat surprising result was found for the lead derivatives (see Fig. 3(c and d)): for Pb(GEH)ClO₄ (compound II) a value of 2.66 ± 0.20 s was obtained, whereas for Pb(GE) (complex III), the value was 1.19 ± 0.12 s. Chelate formation is suggested for the latter complex in terms of its far IR spectrum, as the amino group is coordinated. However, this complex (III) shows splitting in the ^{13}C signals belonging to the β and γ carbon atoms from the glutamic acid residue. Powder X-ray diffraction was performed on all the compounds in order to understand the low value of $\langle T_1 \rangle$ obtained for

Table 5
 Coordination bond lengths (Å) and angles (°) for complex II^a

Bond lengths			
Pb1–O11#1	2.451(6)	Pb1–O10#1	2.571(8)
Pb1–O13#2	2.576(19)	Pb1–O15	2.593(7)
Pb1–O14	2.657(8)	Pb1–O13	2.734(19)
Bond angles			
O11#1–Pb1–O10#1	51.3(4)	O11#1–Pb1–O13#2	77.2(6)
O10#1–Pb1–O13#2	118.0(3)	O11#1–Pb1–O15	82.1(3)
O10#1–Pb1–O15	69.6(3)	O13#2–Pb1–O15	71.6(3)
O11#1–Pb1–O14	78.8(3)	O10#1–Pb1–O14	108.5(3)
O13#2–Pb1–O14	89.5(3)	O15–Pb1–O14	155.7(2)
O11#1–Pb1–O13	81.9(6)	O10#1–Pb1–O13	74.2(3)
O13#2–Pb1–O13	135.9(2)	O15–Pb1–O13	142.8(3)
O14–Pb1–O13	48.2(3)		

^a Symmetry transformations used to generate equivalent atoms: #1, $-x+3/2, y-1/2, -z+1$; #2, $x, y-1, z$; #3, $-x+3/2, y+1/2, -z+1$; #4, $x, y+1, z$; #5, $-x+2, y, -z+1$.

this compound where a more rigid bonded form of the ligand was expected. All compounds show a high degree of crystallinity except compound III, where a remarkable presence of amorphous material was found. These results are consistent with the presence of lead oxide in this product, according to the elemental analysis.

$\langle T_1 \rangle$ determination was also carried out for Zn(GE) (compound VI) in order to complete the data yielding a $\langle T_1 \rangle$ value of 4.62 ± 0.22 s. However, no comparison could be made, as the protonated-ligand derivative was not isolated. We have found no information regarding the viability of comparing this parameter between complexes of different metal centers.

Table 4
 Signals assigned to the Metal–amino interaction

Compound	Original sample M–NH ₂ (cm ⁻¹)	Expected upon deuteration (cm ⁻¹)	Observed in deuterated sample M–ND ₂ (cm ⁻¹)
III. Pb(GE)	338.9	320.93	318.6
IV. Cd(GE)	360.3	342.28	343.1
VI. Zn(GE)	364.5	347.83	350.6

Table 6
Coordination bond lengths (Å) and angles (°) for complex V^a

Bond lengths			
Cd1–O11#1	2.351(2)	Cd1–O11#2	2.351(2)
Cd1–O14#3	2.416(2)	Cd1–O14	2.416(2)
Cd1–O13#3	2.449(2)	Cd1–O13	2.449(2)
Cd1–O10#2	2.491(2)	Cd1–O10#1	2.491(2)
Bond angles			
O11#1–Cd1–O11#2	120.17(12)	O11#1–Cd1–O14#3	117.59(8)
O11#2–Cd1–O14#3	94.62(7)	O11#1–Cd1–O14	94.62(7)
O11#2–Cd1–O14	117.59(8)	O14#3–Cd1–O14	113.94(11)
O11#1–Cd1–O13#3	82.54(8)	O11#2–Cd1–O13#3	148.15(7)
O14#3–Cd1–O13#3	53.66(6)	O14–Cd1–O13#3	78.83(9)
O11#1–Cd1–O13	148.15(7)	O11#2–Cd1–O13	82.54(8)
O14#3–Cd1–O13	78.83(9)	O14–Cd1–O13	53.66(6)
O13#3–Cd1–O13	87.67(13)	O11#1–Cd1–O10#2	84.73(8)
O11#2–Cd1–O10#2	53.27(7)	O14#3–Cd1–O10#2	147.87(6)
O14–Cd1–O10#2	84.66(8)	O13#3–Cd1–O10#2	158.20(7)
O13–Cd1–O10#2	93.97(9)	O11#1–Cd1–O10#1	53.27(7)
O11#2–Cd1–O10#1	84.73(8)	O14#3–Cd1–O10#1	84.66(8)
O14–Cd1–O10#1	147.87(6)	O13#3–Cd1–O10#1	93.97(9)
O13–Cd1–O10#1	158.20(7)	O10#2–Cd1–O10#1	92.50(12)

^a Symmetry transformations used to generate equivalent atoms, #1, $-x+1, -x+y+1, -z+5/3$; #2, $-y, x-y-1, z-1/3$; #3, $x-y, -y, -z+4/3$; #4, $-x+y+1, -x, z+1/3$.

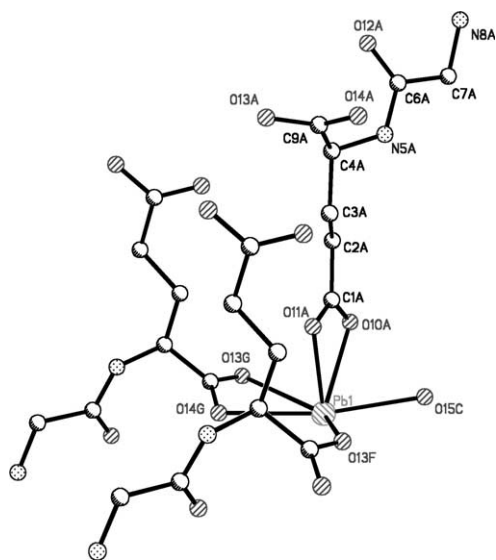


Fig. 4. The coordination environment for Pb atoms in **II**. Thermal ellipsoids are at 50% probability level. H atoms are omitted for clarity. Symmetry codes used to generate equivalent atoms are the following, (A) $3/2-x, -1/2+y, 1-z$; (B) $x, y-1, z$.

3.3. Infrared spectra

3.3.1. Mid and far IR spectra

As expected, IR spectra of those complexes known to be formed by the protonated peptide (GEH^+ : **II** and **V**) show the pattern of a primary ammonium group in the $3000\text{--}2500\text{ cm}^{-1}$ region, while those of the deprotonated peptide (GE^{2-} : **III**, **IV** and **VI**) show a 3 band pattern from 3400 to 3000 cm^{-1} as well as the

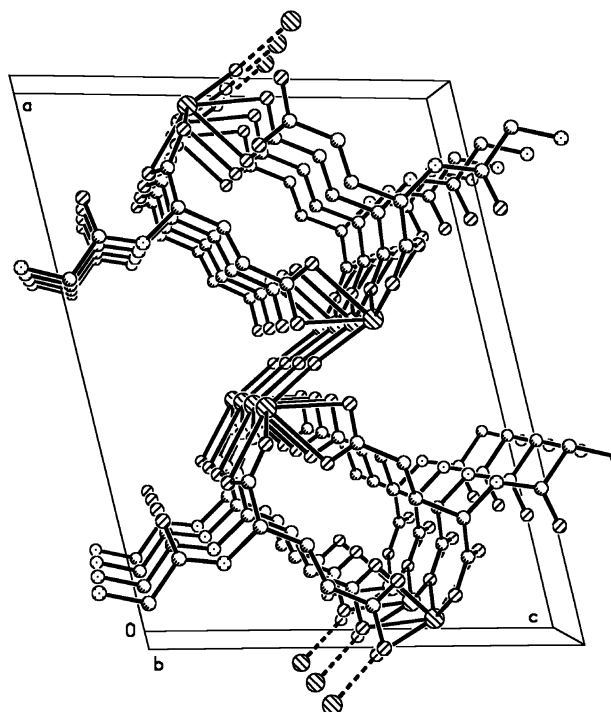


Fig. 5. The 3D polymeric structure of **II** viewed along the $[010]$ axis. H atoms are omitted for clarity. Perchlorate anions (not shown) lie on the left and right sides of the bridging water molecules.

corresponding NH amide band around 3350 cm^{-1} . All these bands show an approximate 800 cm^{-1} lower energy shift upon deuteration, as expected according to reduced mass calculations for the isotopomers.

The far IR spectra recorded for the GE^{2-} derivatives (**III**, **IV** and **VI**) show bands which suggest $\text{M-NH}_2\text{R}$ interaction (see Table 4) that are absent in the spectra of **II** and **V**, known to have the ammonium group by X-ray diffraction and mid IR studies. Upon deuteration, these bands also shift to lower energy values that are in excellent agreement with reduced mass calculations. These results are consistent with our previous observations in lead aspartate complexes [6a].

Absence of bands in this region in the spectrum of the calcium derivative further supports our assumption of an ionic behavior.

3.4. Crystallography

Coordination bond distances and angles are displayed in Table 5 for **II** and in Table 6 for **V**. The geometry for the ligand GEH in both structures does not present unusual features. For **II**, the metal center is 6-coordinated: two different carboxylate groups from two symmetry equivalent GEH ligands are bonded to the Pb ion, with the O13 atom μ_3 -coordinated, forming a 2D network with base vectors $[010]$ and $[001]$. This substructure is then based on 16-membered rings containing two Pb ions and two GEH ligands (Fig. 5). The sphere

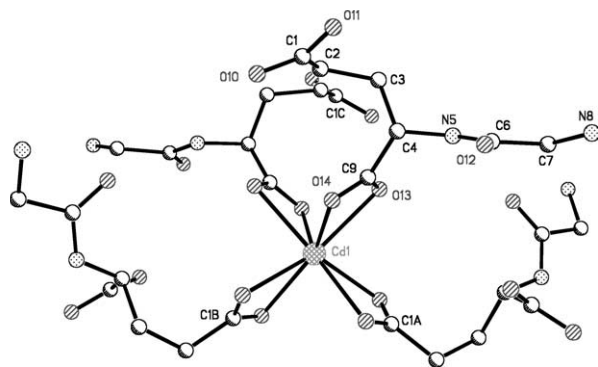


Fig. 6. The coordination environment for Cd atoms in **V**. Thermal ellipsoids are at 50% probability level. H atoms are omitted for clarity. Symmetry codes used to generate equivalent atoms are the following, (A) $1-x, 1-x+y, 5/3-z$; (B) $-y, -1+x-y, -1/3+z$; (C) $x-y, -y, 4/3-z$.

of coordination is completed by a water molecule (O15, lying on the binary axis of the $C2$ space group), which bridges two symmetry related Pb atoms and allows for the formation of a 3D polymeric structure, the third base vector being [100] (see Fig. 5). The resulting $[PbO_6]$ coordination sphere (Fig. 4) is best described as distorted square pyramidal, where the apical position is occupied by the carboxylate oxygen atoms (O10, O11). Distortion from an ideal geometry mainly arises from the bite angles of the carboxylate groups, $51.3(4)$ and $48.2(3)^\circ$, and from the long Pb1- μ_3 O13 distance, $2.734(19)$ Å. This coordination geometry is reminiscent of that previously reported [6a] for a similar 3D polymer, $Pb(aspH)(NO_3)$. Particularly noteworthy is the space below the plane of the pyramid, where the stereochemically active lone pair of Pb is probably localized. However, a striking feature differentiating **II** and $Pb(aspH)(NO_3)$ is that the Pb atom lies 0.42 Å below the base of the pyramid for **II**, while this metal lies 0.13 Å above the base of the pyramid in the latter case. There is no contribution from the perchlorate anions to the polymeric structure.

A very different structure is obtained for **V** for many reasons, (i) metal–ligand ratio is 1:2 for **V** but 1:1 for **II** (see Section 2); (ii) in spite of the presence of water molecules in the crystal, these do not coordinate to the metal. (iii) the nature of the metal seems to be essential, related to the presence of a lone pair for the Pb(II) ion but not for Cd(II). For **V**, four symmetry related GEH ligands are bonded to the metal center, through the 3_2 screw-axis of the trigonal space group. Two ligands coordinate through the (O10, O11) carboxylate and the remaining two through (O13, O14). The co-ordination sphere (see Fig. 6) can be described as a severely distorted square antiprism. The distortion is due to the restriction of the bite angles of the carboxylate groups, $53.27(7)$ and $53.66(6)^\circ$, rather than disparity in the bond distances, which span the short range of $2.351(2)$ –

$2.491(2)$ Å. In comparison with **II**, no μ_3 -O atoms or bridging water molecules are needed in order to form a 3D polymer, with base vectors [100], [010] and [001] (not shown). Disordered water molecules are located near the origin of the cell, filling the voids of the inorganic polymer.

In both complexes, nitrogen-containing groups of GEH are not involved in the polymeric structures. However, the observed 3D arrangements are possible because of the similar coordination ability of the two carboxylate groups in GEH, pointing to different directions in space. The resulting structures are exceptionally compact compared with others in the field of inorganic polymers [21]: calculated packing indexes [22] are 77.9 and 75.5% for **II** and **V**, respectively.

The affinity of the protonated dipeptide toward calcium is remarkable when compared with the other cations. This is unusual for mono and bidentate oxygen donors [23]. For calcium the ligand can act as an O, O donor at the most whereas for the other cations it reflects the trend already reported by Martin [24], where an O, O donor has a higher affinity toward lead, then zinc and then cadmium. When the ligand loses the ammonium proton, and behaves as an O, N donor, the expected trend of formation constant $Zn > Pb > Cd \gg Ca$ is observed. The higher affinity of Cd^{2+} and Zn^{2+} toward nitrogen is reflected in the isolable compounds and in the formation constants. These observations are consistent with Pearson's Hard and Soft Acids and Bases principle.

4. Supplementary material

Crystallographic data for the structural analysis have been deposited with the Cambridge Crystallographic Data Centre, CCDC Nos. 173243 (**II**) and 173244 (**IV**). Copies of this information may be obtained free of charge from the Director, CCDC, 12 Union Road, Cambridge CB2 1EZ, UK (fax: +44-1233-336-033; e-mail: deposit@ccdc.cam.ac.uk or www: <http://www.ccdc.cam.ac.uk>). Structure factors (CIF format) are available on request from the authors.

Acknowledgements

We thank CONACyT for sponsoring this project (Grant 4913-E9406). S.B. is grateful to CONACyT for financial support (programa de retención, 000027).

References

- [1] (a) S. Forsén, J. Kördel, Calcium in biological systems, in: I. Bertini, H.B. Gray, S.J. Lippard, J.S. Valentine (Eds.), *Bioinor-*

- ganic Chemistry, University Science Books, Herndon, VA, 1994, p. 123;
- (b) S. Linse, S. Forsén, *Adv. Second Messenger Phosphoprot. Res.* 30 (1995) 89.
- [2] C.S. Fullmer, S. Edelstein, R. Wasserman, *J. Biol. Chem.* 260 (1985) 6816.
- [3] (a) S.I. Koo, C.S. Fullmer, R.H. Wasserman, *J. Nutr.* 110 (1980) 1813;
- (b) J.E.D. Bogden, S.B. Gertner, S. Christakos, F.W. Kemp, Z. Yang, S.R. Katz, C. Chu, *J. Nutr.* 122 (1992) 1351;
- (c) R.A. Corradino, C.S. Fullmer, *Arch. Biochem. Biophys.* 199 (1980) 43.
- [4] (a) R.A. Corradino, C.S. Fullmer, *Arch. Biochem. Biophys.* 199 (1980) 43;
- (b) S.I. Koo, C.S. Fullmer, R.H. Wasserman, *J. Nutr.* 108 (1978) 1813;
- (c) C.S. Fullmer, T. Oku, R.H. Wasserman, *Environ. Res.* 22 (1980) 386;
- (d) P. Washko, R.J. Cousins, *J. Nutr.* 107 (1977) 920;
- (e) P. Washko, R.J. Cousins, *J. Toxicol. Environ. Health* 1 (1976) 1055;
- (f) A.A. Van Barneveld, C.J. Van der Hamer, *Toxicol. Appl. Pharmacol.* 79 (1985) 1.
- [5] (a) S. Linse, W.J. Chazin, *Protein Sci.* 4 (1995) 1038;
- (b) W. Chazin, T.D. Veenstra, *Rapid Commun. Mass. Spectrom.* 13 (1999) 548;
- (c) M. Akke, N. Skelton, J. Kordel, A.G. Palmer, W.J. Chazin, *Biochemistry* 32 (1993) 9832;
- (d) N. Skelton, J. Koerdel, M. Akke, W.J. Chazin, *J. Mol. Biol.* 227 (1992) 1100;
- (e) M. Akke, S. Forsén, W.J. Chazin, *J. Mol. Biol.* 252 (1995) 102;
- (f) J. Matysik, G. Alia, Nachtegaal, H.J. van Gorkom, A.J. Hoff, H.J.M. de Groot, *Biochem.* 39 (2000) 6751.
- [6] (a) L. Gasque, S. Bernès, R. Ferrari, C.R. de Barbarin, M.J. Gutiérrez, G. Mendoza-Díaz, *Polyhedron* 19 (2000) 649;
- (b) L. Gasque, S. Bernès, R. Ferrari, G. Mendoza-Díaz, *Polyhedron* 21 (2002) 935.
- [7] D.M.E. Szebenyi, S.K. Obendorf, K. Moffat, *Nature* 294 (1981) 327.
- [8] R.F. Jameson, M.F. Wilson, *J. Chemical Society, Dalton Trans.* (1972) 2607.
- [9] P. Gans, A. Sabatini, A. Vacca, *HYPERQUAD*, 2000.
- [10] I. Puigdomenech; *MEDUSA*, 1998.
- [11] J. Fait, *XSCANS* (release 2.21) Users Manual, Siemens Analytical X-ray Instruments Inc, Madison, WI, 1996.
- [12] (a) G.M. Sheldrick, *SHELXTL-PLUS*, release 5.10, Siemens Analytical X-ray Instruments Inc, Madison, WI, 1998;
- (b) G.M. Sheldrick, *SHELX97* Users Manual, University of Göttingen, Göttingen, Germany, 1997.
- [13] (a) H.D. Flack, *Acta Crystallogr.*, A 39 (1983) 876;
- (b) G. Bernardinelli, H.D. Flack, *Acta Crystallogr.*, Sect. A 41 (1985) 500.
- [14] Gergely, A, Farkas, E., *J. Chem. Soc., Dalton Trans.* (1982) 381.
- [15] P.G. Mennitt, M.P. Shatlock, V.J. Bartuska, G.E. Maciel, *J. Phys. Chem.* 85 (1981) 2087.
- [16] T. Takayama, S. Ohuchida, Y. Koike, M. Watanabe, D. Hashizume, Y. Ohashi, *Bull. Chem. Soc. Jpn.* 69 (1996) 1579.
- [17] M.F. Summers, *Coord. Chem. Rev.* 86 (1988) 43.
- [18] P.J. Barrie, A. Gyani, M. Motevalli, P. O'Brien, *Inorg. Chem.* 32 (1993) 3862.
- [19] H.O. Kalinowski, S. Berger, S. Braun, *Carbon-13 NMR Spectroscopy*, Wiley, Chichester, UK, 1988, p. 228.
- [20] A.D. Irwin, C.D. Chendler, R. Assink, M.J. Hampden-Smith, *Inorg. Chem.* 33 (1994) 100.
- [21] Examples for Cd(II) polymers: (a) A.B. Corradi, L. Menabue, M. Saladini, M. Sola, L.P. Battaglia, *J. Chem. Soc., Dalton Trans.* (1992) 2623;
- (b) J. Yamada, H. Hashimoto, Y. Inomata, T. Takeuchi, *Bull. Chem. Soc. Jpn.* 67 (1994) 3224;
- (c) H.C. López-Sandoval, N. Barba-Behrens, S. Bernès, N. Farfan-García, H. Höpfl, *J. Chem. Soc., Dalton Trans.* (1997) 3415 and references cited therein.
- [22] A.L. Spek, *PLATON*, A Multipurpose Crystallographic Tool, Utrecht University, Utrecht, The Netherlands, 1998.
- [23] A.E. Martell, R.M. Smith, *Critical Stability Constants*, vol. 3, Plenum Press, New York, 1997.
- [24] R.B. Martín, *Bioinorganic chemistry of toxicity*, in: H.G. Seiler, H. Sigel, A. Sigel (Eds.), *Handbook on Toxicity of Inorganic Compounds*, Marcel Dekker, New York, 1988, p. 17.